Microphysics of Air-Sea Exchanges

O. B. Brown
Rosenstiel School of Marine and Atmospheric Science
University of Miami
4600 Rickenbacker Causeway
Miami, FL 33149-1098
Phone: (305) 361-4000 Ffax: (305) 361-4711 Email: obrown@rsmas.miami.edu

R. H. Evans
Rosenstiel School of Marine and Atmospheric Science
University of Miami
4600 Rickenbacker Causeway
Miami, FL 33149-1098
Phone: (305) 361-4799 Fax: (305) 361-4622 Email: revans@rsmas.miami.edu

M. A. Donelan
Rosenstiel School of Marine and Atmospheric Science
University of Miami
4600 Rickenbacker Causeway
Miami, FL 33149-1098
Phone: (305) 361-4717 Fax: (305) 361-4701 Email: mdonelan@rsmas.miami.edu

P. J. Minnett
Rosenstiel School of Marine and Atmospheric Science
University of Miami
4600 Rickenbacker Causeway
Miami, FL 33149-1098
Phone: (305) 361-4104 Fax: (305) 361-4622 Email: pminnett@rsmas.miami.edu

B. Ward
Applied Ocean Physics & Engineering,
Woods Hole Oceanographic Institution
Woods Hole, MA 02543, USA
Phone: (508) 289.3407 Fax: (508) 457.2194 Email: bward@whoi.edu

W. R. McGillis
Applied Ocean Physics & Engineering
Applied Ocean Physics & Engineering,
Woods Hole Oceanographic Institution
Woods Hole, MA 02543, USA
Phone: (508) 289-3325 Fax: (508) 457-2132 Email: wmcgillis@whoi.edu

Award Number: N00014-03-1-0384
http://www.rsmas.miami.edu/groups/rsg.html

Report Documentation Page

Form Approved
OMB No. 0704-0188

1. REPORT DATE	2. REPORT TYPE	3. DATES COVERED
30 SEP 2003		**00-00-2003 to 00-00-2003**

4. TITLE AND SUBTITLE	5a. CONTRACT NUMBER
Microphysics of Air-Sea Exchanges	5b. GRANT NUMBER
	5c. PROGRAM ELEMENT NUMBER
6. AUTHOR(S)	5d. PROJECT NUMBER
	5e. TASK NUMBER
	5f. WORK UNIT NUMBER
7. PERFORMING ORGANIZATION NAME(S) AND ADDRESS(ES) **Rosenstiel School of Marine and Atmospheric Science,,University of Miami,4600 Rickenbacker Causeway,,Miami,,FL, 33149**	8. PERFORMING ORGANIZATION REPORT NUMBER
9. SPONSORING/MONITORING AGENCY NAME(S) AND ADDRESS(ES)	10. SPONSOR/MONITOR'S ACRONYM(S)
	11. SPONSOR/MONITOR'S REPORT NUMBER(S)

12. DISTRIBUTION/AVAILABILITY STATEMENT
Approved for public release; distribution unlimited

13. SUPPLEMENTARY NOTES

14. ABSTRACT

The research efforts are targeted at improving our understanding of the microphysics of air-sea exchanges, especially the physics of the oceanic thermal skin and diurnally-influenced layers. This will lead to better assimilation of satellite-derived sea-surface temperature (SST) fields into meaningful climatologies and to more physically-based applications of satellite data to studies of air-sea interactions and to other naval applications. The constellation of satellites with infrared radiometers for SST measurements has a range of local over-pass times and, because of the diurnally forced fluctuation in SST and of the fluctuations of the skin effect in response to differing air-sea fluxes, this creates a problem in combining these fields into a reliable, consistent composite analysis. The results of this new research will improve the reliability of such composite analyses for naval applications.

15. SUBJECT TERMS

16. SECURITY CLASSIFICATION OF:			17. LIMITATION OF ABSTRACT	18. NUMBER OF PAGES	19a. NAME OF RESPONSIBLE PERSON
a. REPORT	b. ABSTRACT	c. THIS PAGE			
unclassified	**unclassified**	**unclassified**	**Same as Report (SAR)**	**8**	

LONG-TERM GOALS

The research efforts are targeted at improving our understanding of the microphysics of air-sea exchanges, especially the physics of the oceanic thermal skin and diurnally-influenced layers. This will lead to better assimilation of satellite-derived sea-surface temperature (SST) fields into meaningful climatologies and to more physically-based applications of satellite data to studies of air-sea interactions and to other naval applications. The constellation of satellites with infrared radiometers for SST measurements has a range of local over-pass times and, because of the diurnally forced fluctuation in SST and of the fluctuations of the skin effect in response to differing air-sea fluxes, this creates a problem in combining these fields into a reliable, consistent composite analysis. The results of this new research will improve the reliability of such composite analyses for naval applications.

OBJECTIVES

The objectives are to achieve a better understanding of the physics of the near-surface temperature gradients; specifically how they respond to different flux and wind regimes. This improved knowledge will be applied to providing a better, physically-based approach to time-compositing SST fields derived from infrared imaging radiometers on earth observation satellites.

APPROACH

A comprehensive set of measurements were taken in the new Air-Sea Interaction Saltwater Tank (ASIST) at RSMAS under controlled conditions of wind speed and air-sea temperature difference to examine the behavior of the thermal skin layer. The measurements are comprehensive both in the extensive instrumentation brought to the experiments, and the wide range of imposed parameters.

WORK COMPLETED

A set of ASIST experiments were done in December 2001. Fresh water was used and the wind tunnel was in the open mode to allow steady state fluxes to be established. The experiment covered air-sea temperature differences from -15K to +15K, and wind speeds from 0 to 10ms^{-1}. All of the parameters that influence the thermal skin layer were measured directly in the ASIST with uncertainties <5%.

The skin temperature was measured using the M-AERI (Minnett et al. 2001) looking down into flume, and two infrared imagers were mounted above the flume; one was operated by Dr G. Smith of NRL, as part of collaborative research, and the other was a new sensor at RSMAS funded from another grant. A full description of the experimental set-up and measurement procedure can be found in the Annual Report for last year. The activities on the current year have focused on the processing, quality control and analysis of the measurements.

RESULTS

We are concerned with the mixing characteristics of the upper layer of the ocean and particularly with the very thin layer adjacent to the surface, in which rapid changes of temperature and dissolved contaminants distinguish it from the relatively well-mixed surface layers beneath. The wind acting on the surface provides the source of mechanical energy that mixes the upper layers, either through the breakdown of the shear layer generated by the tangential stress or through the direct injection of turbulence from the breaking of waves at and above the spectral peak of the wind-generated sea. The

latter process has been shown to dominate once the wind speed exceeds the level of "incipient white-capping" or about 6 ms^{-1} at 10m height. Several field experiments have shown a sudden increase in the mass transfer velocity of slightly soluble contaminants when the wind exceeds this limit, and laboratory experiments have linked mass transfer velocity and mean square slope (*mss*) of the waves. Of course, the *mss* does not directly mix the surface fluid but it may be an effective indicator of the rate of wave breaking and therefore the kinetic energy dissipation rate induced by wave breaking.

Our measurements permit us to examine the connection between *mss* and turbulent kinetic energy dissipation, ε. The *mss* was estimated from surface elevation measurements at three points obtained with the aid of a laser elevation gauge (LEG). The LEG measures the surface elevation at a point by tracking the intersection of a laser beam with the surface using a line scan digital camera. A small quantity of fluorescein in the water, causes laser-induced fluorescence a distinct change in the scattered light above and below the surface. The LEGs have a resolution/accuracy of about 0.3mm. The three laser beams, being about 1mm in diameter at the surface are arranged in an equilateral triangle of side 1cm, so that the slopes of waves of wavelengths 2cm and greater can be obtained.

The measurements of ε were obtained with hot-film anemometry at a depth of 6cm. A miniature wedge probe was overheated by about 10 K and recorded at 200 Hz. The level of the spectrum of the downstream component of velocity in its inertial sub-range just below the wave peak was used to estimate ε. Figure 1 compares the *mss* with ε [m^2s^{-3}]. The solid line represents $\varepsilon = 0.0545\ mss^2$ and is almost indistinguishable from the (dashed) linear regression line in logarithmic coordinates.

To make a physically meaningful connection between *mss* and ε we note that the latter reflects the loss of energy from the wave field through breaking, whereas *mss* may be a good statistical measure of the incidence of breaking (steep waves) per unit area. The energy lost in each breaking event is therefore related to the loss of potential energy from the crest of the breaker or *gh*, where *h* is the crest height. Since wave breaking occurs in a very narrow range of slopes, the energy loss per breaker may be expressed in terms of the wavelength (λ) of the breaking wave: *g*λ. The rate of breaking for a given *mss* will depend on the frequency of the breaking wave, ω as was shown by Donelan et al. 1972. Consequently the rate of energy loss from breaking, É, may be expressed in terms of these variables:

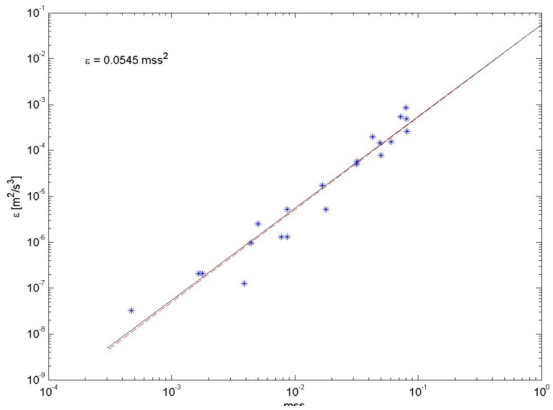

Figure 1. Measured turbulent kinetic energy dissipation, ε vs mean square slope of the waves, mss.

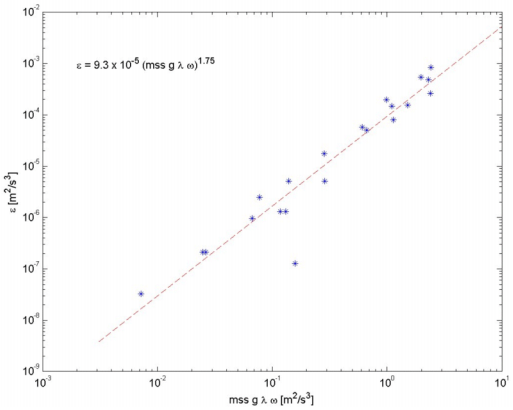

Figure 2. ε vs mss with dimensional consistency provided by the gravitational acceleration and the relevant wave properties: wavelength, λ and radian frequency, ω.

$$É \sim mss\ g\ \lambda\ \omega$$

Figure 2 shows the correlation between É and the measured ε at 6cm depth:

$$\varepsilon = 9.3 \times 10^{-5}\ (mss\ g\ \lambda\ \omega)^{1.75}$$

The Imaging Slope Gauge (ISG) used a uniform light source underneath the test section shone through a mask with known gradients in red, green and blue intensities. The light then passed through a Fresnel lens that focused all light that has the same slope on the same point of the mask. This then allowed an RGB camera to directly observe the water surface slope through the relative intensities of the three color components at each point of the image. The ISG imaged an area of the water surface of up to 45 cm (downwind) x 30 cm (crosswind) at a resolution of 640 x 240. These images are sampled at a rate of 120 Hz using two interleaved RBG cameras. Collection of images was triggered by the M-AERI acquisition cycle and continued for a period of 4 seconds for each run. The total mean square slope of all images at all pixels for each run was compared with the wind speed (Figure 3). Although there was considerable scatter the general trend was a linear increase with wind speed above 2 ms^{-1} as expected. The spatial distribution of the slopes was typically randomly distributed about the mean value. However, for several of the runs there were spatially inhomogeneous mean square slopes (Figure 4). Bands of alternating high and low mean square slopes were observed aligned with the wind direction.

High-resolution thermometric measurements were conducted with the microthermometer, capable of resolving the viscous boundary layer. Figure 5 shows three consecutive runs taken under similar heat flux conditions, with the heat flux into the water. In Figure 5a the wind speed was 1 ms^{-1} and the thermometric measurements show a ΔT of 0.3 K. The conditions reflect a nighttime situation, with the absence of any stratification in the water column. In Figure 5b the wind speed is at 3 ms^{-1} , and the thermometric ΔT is reduced to about 0.15 K. The wind speed is increased to 5 ms^{-1} (Figure 5c), and the average water temperature has decreased by 0.8 K i.e. from about 14.3 to about 13.5 ºC. The microthermometer ΔT is about 0.08 K.

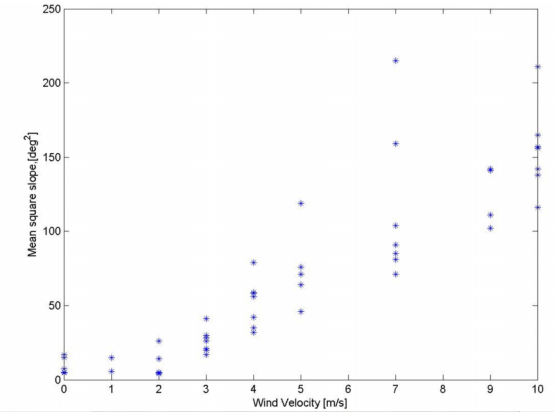

Figure 3. Mean Square along-tank slope as observed by the Imaging Slope Gauge. MSS given in units of deg^2. The air-sea temperature difference varies from -15 to +15 K for these runs.

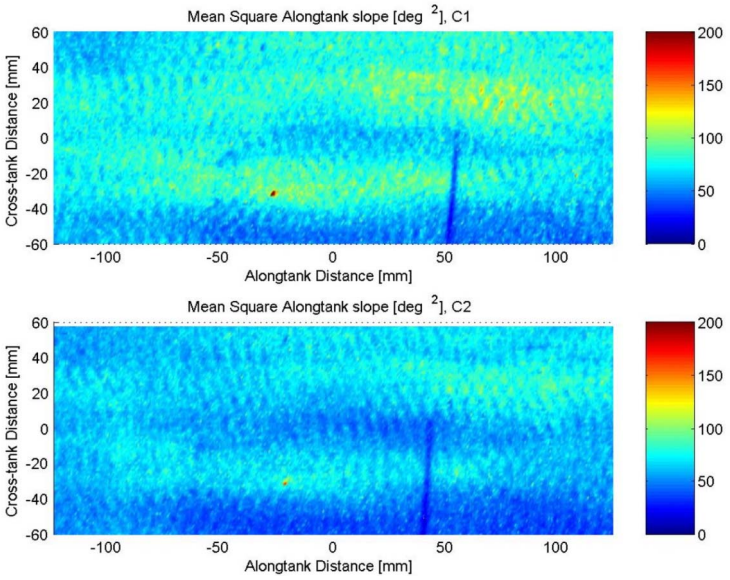

Figure 4. Mean square along-tank slope at each pixel as observed by the ISG. Wind speed was 4 ms^{-1} from right to left in these images. $T_{air} - T_{sea}$ was -10 K. The line in the image is due to either a scratch or a wrinkle in the film covering the opening.

The temperature drop across the molecular boundary layer is linear with depth, and a straight line through the temperature drop shows a boundary layer thickness of about 2 mm for the lowest wind speed. For the two higher wind speeds, the thickness of the sub-layer is approximately 1 mm. The fact that the thickness does not scale with wind speed may be due to the small heat flux increase in run 12 with the decrease in water temperature.

Figure 6 shows a different situation, where the direction of the heat flux is out of the water providing a cooler skin than the bulk. However, the absolute value of the air-water temperature difference is smaller than the situation presented in figure 5, and the wind speeds are higher. The microthermometer ΔTs are 0.2 K, 0.17 K, 0.05 K, and 0.05 K, respectively. During these four runs, the M-AERI skin temperature remains invariant at 30.2 ºC, whereas the average bulk temperature varies by a few tenths of a degree.

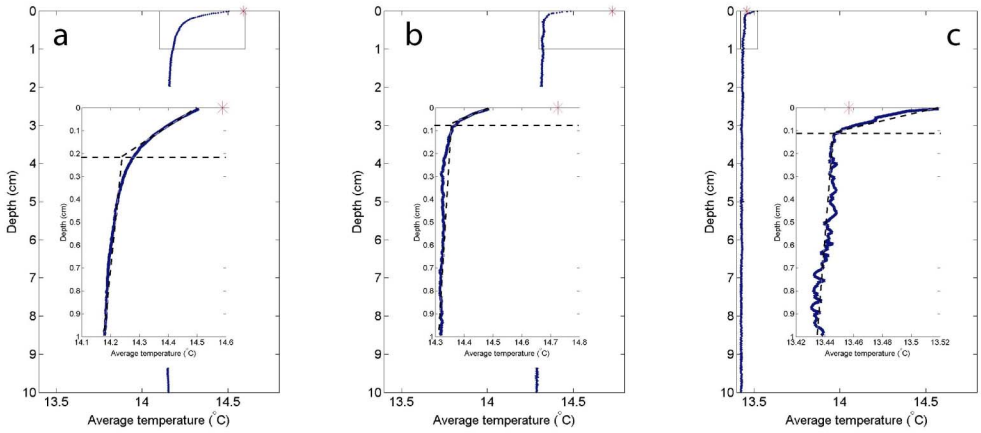

Figure 5. Averaged temperature profiles taken with air-water temperature difference of +10 K. The wind speeds were 1, 3, and 5 ms^{-1}, respectively. The overlaid plot in each subplot is that of the upper 10mm denoted by the box. The asterisk in each subplot represents the M-AERI skin temperature.

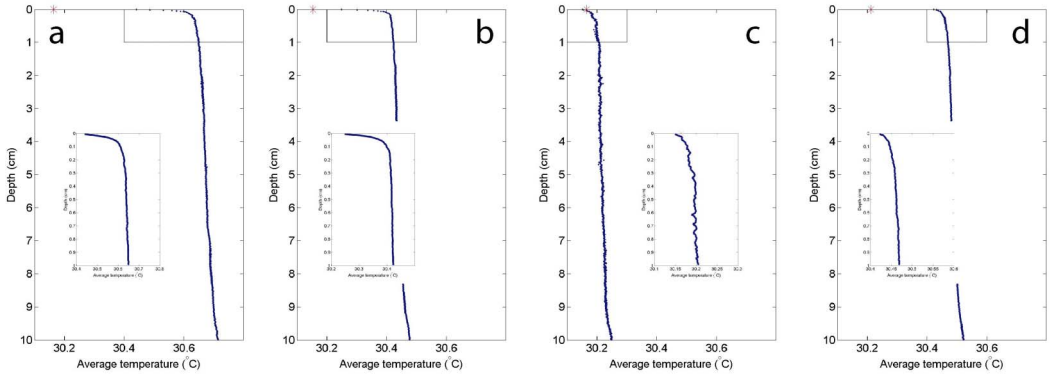

Figure 6. Averaged temperature profiles taken with air-water temperature difference of -5 K. The wind speeds were 4, 5, 7, and 10 ms^{-1}, respectively.

IMPACT/APPLICATIONS

The research is directed toward better understanding of the physics of the skin layer which will allow improved compositing of SST fields derived form space borne sensors with different overpass times, and more physical models relating the skin and sub-surface bulk temperatures.

TRANSITIONS

Collaborative work with NAVOCEANO continues with RSMAS providing guidance in algorithm development and improvements that come from the continuing AVHRR Pathfinder studies, and NAVOCEANO providing near-real time *in-situ* data from ocean buoys.

RELATED PROJECTS

This project has benefited from related research being done in the Remote Sensing Group at RSMAS with funding from other federal agencies, specifically instrument development through contracts and grants from NASA and NOAA. The ASIST facility was developed with funding from ONR, DURIP.

REFERENCES

Donelan, M. A., M. S. Longuet-Higgins and J. S. Turner (1972). "Whitecaps." Nature **239**: 449-451

Minnett, P. J., R. O. Knuteson, F. A. Best, B. J. Osborne, J. A. Hanafin and O. B. Brown (2001). "The Marine-Atmospheric Emitted Radiance Interferometer (M-AERI), a high-accuracy, sea-going infrared spectroradiometer." Journal of Atmospheric and Oceanic Technology **18**(6): 994-1013